


Received: 3 June 2019 | Revised: 13 October 2019 | Accepted: 1 November 2019

DOI: 10.1002/hbm.24861

## RESEARCH ARTICLE

WILEY

# Getting into sync: Data-driven analyses reveal patterns of neural coupling that distinguish among different social exchanges

Beáta Špiláková<sup>1,3</sup>  | Daniel J. Shaw<sup>1,4</sup> | Kristína Czekóová<sup>1</sup> |  
Radek Mareček<sup>2,3</sup> | Milan Brázdil<sup>1,3</sup>

<sup>1</sup>Behavioural and Social Neuroscience Research Group, CEITEC—Central European Institute of Technology, Masaryk University, Brno, Czech Republic

<sup>2</sup>Multimodal and Functional Neuroimaging Laboratory, CEITEC—Central European Institute of Technology, Masaryk University, Brno, Czech Republic

<sup>3</sup>Department of Neurology, Faculty of Medicine, Masaryk University, Brno, Czech Republic

<sup>4</sup>Department of Psychology, School of Life and Health Sciences, Aston University, Birmingham, UK

**Correspondence**

Daniel J. Shaw, Department of Psychology, School of Life and Health Sciences, Aston University, Birmingham B4 7ET, UK.  
Email: d.shaw1@aston.ac.uk

**Funding information**

Grantová Agentura České Republiky, Grant/Award Number: GA18-21791S; MEYS; Central European Institute of Technology; Czech Science Foundation; Ministry of Education, Youth and Sports; European Regional Development Fund

**Abstract**

In social interactions, each individual's brain drives an action that, in turn, elicits systematic neural responses in their partner that drive a reaction. Consequently, the brain responses of both interactants become temporally contingent upon one another through the actions they generate, and different interaction dynamics will be underpinned by distinct forms of between-brain coupling. In this study, we investigated this by “performing functional magnetic resonance imaging on two individuals simultaneously (dual-fMRI) while they competed or cooperated with one another in a turn-based or concurrent fashion.” To assess whether distinct patterns of neural coupling were associated with these different interactions, we combined two data-driven, model-free analytical techniques: group-independent component analysis and inter-subject correlation. This revealed four distinct patterns of brain responses that were temporally aligned between interactants: one emerged during co-operative exchanges and encompassed brain regions involved in social cognitive processing, such as the temporo-parietal cortex. The other three were associated with competitive exchanges and comprised brain systems implicated in visuo-motor processing and social decision-making, including the cerebellum and anterior cingulate cortex. Interestingly, neural coupling was significantly stronger in concurrent relative to turn-based exchanges. These results demonstrate the utility of data-driven approaches applied to “dual-fMRI” data in elucidating the interpersonal neural processes that give rise to the two-in-one dynamic characterizing social interaction.

**KEYWORDS**

competition, co-operation, hyperscanning, interaction structure, inter-subject correlation, neural coupling, social interaction

## 1 | INTRODUCTION

Social interactions unfold as a two-in-one dynamic (Koike, Tanabe, & Sadato, 2015; Redcay & Schilbach, 2019), whereby each individual's behavior is simultaneously an antecedent to and a consequence of

their interaction partners' actions. At the level of the brain, this emerges through an indirect chain of interpersonal neural events; one interactant's brain responses initiate an action that, in turn, elicits systematic neural responses in their partner to drive a reaction. In this light, the particular dynamic of an interaction emerges through a

This is an open access article under the terms of the Creative Commons Attribution-NonCommercial License, which permits use, distribution and reproduction in any medium, provided the original work is properly cited and is not used for commercial purposes.

© 2019 The Authors. *Human Brain Mapping* published by Wiley Periodicals, Inc.

reciprocal process of between-brain contingencies, or “neural coupling” (Hasson & Frith, 2016). Elucidating the patterns of neural coupling that underlie different forms of social exchange might therefore provide an interpersonal neural substrate of interactive behavior, but this requires the development of new paradigms and analytical techniques for social neuroscience research (Hasson & Honey, 2012; Schilbach et al., 2013; Zaki, Bolger, & Ochsner, 2008). In response to this, a new wave of “two-person” or “in situ” social neuroscience has emerged (Hari, Himberg, Nummenmaa, Hämäläinen, & Parkkonen, 2013; Kasai, Fukuda, Yahata, Morita, & Fujii, 2015; Redcay & Schilbach, 2019; Schilbach et al., 2013), whereby the brains of two or more individuals are measured simultaneously while they interact with one another. Such “hyperscanning” allows researchers to explore how social interactions take shape through real-time processes of interpersonal neural coupling.

Hyperscanning has been performed successfully with functional magnetic resonance imaging (fMRI), electroencephalography (EEG), functional near-infrared spectroscopy, and magnetoencephalography (for reviews, see Babiloni & Astolfi, 2014; Scholkmann et al., 2013). With these techniques, studies have revealed various patterns of neural coupling elicited during social interaction; while temporally contingent brain responses are observed between interactants during verbal and non-verbal communication (Ahn et al., 2017; Bilek et al., 2015; Pérez, Carreiras, & Duñabeitia, 2017), between-brain synchrony or “alignment” (Hasson & Frith, 2016) is reported during cooperative and competitive joint-action tasks (e.g., Cheng, Li, & Hu, 2015; Sängler, Müller, & Lindenberger, 2012; Shaw et al., 2018; Toppi et al., 2016). Interestingly, brain regions implicated in social cognitive processes feature frequently in patterns of neural coupling across various types of social interaction, presumably reflecting the mutual recruitment of mechanisms that permit the transmission and encoding of social information. Within the temporo-parietal junction (TPJ), for example, brain responses become synchronized and/or contingent between interactants during economic exchanges (Jahng, Kralik, Hwang, & Jeong, 2017; Tang et al., 2016; Zhang, Liu, Pelowski, Jia, & Yu, 2017), verbal and non-verbal communication (Bilek et al., 2015, 2017; Kinreich, Djalovski, Kraus, Louzoun, & Feldman, 2017; Rojiani, Zhang, Noah, & Hirsch, 2018; Wilson, Molnar-Szakacs, & Iacoboni, 2008), and cooperative joint-action tasks (Abe et al., 2019). This is perhaps unsurprising given the putative role of the TPJ in inferring the intentional and motivational states of others (Bardi, Six, & Brass, 2017; Carlson, Koenig, & Harms, 2013; Eddy, 2016; Frith & Frith, 2006), a process that is essential for interacting successfully with others.

Experimental paradigms employed in hyperscanning studies often confound multiple forms of social exchange, however, making it impossible to identify the discrete patterns of neural coupling associated with different types of interactive behavior. In a theoretical framework proposed by Liu and Pelowski (2014), social interaction is suggested to comprise three distinct dimensions: interaction structure (concurrent or turn-based actions), goal structure (cooperative or competitive goals), and task structure (tasks achieved independently or interdependently). As such, to advance our understanding of how different patterns of neural coupling give rise to interactive behavior, we must first delineate among these dissociable dimensions (Konvalinka & Roepstorff, 2012).

Recently, our team adapted for hyperscanning research, an interactive task capable of such delineation, in which pairs of players either cooperate or compete with one another in a turn-based or concurrent manner to reconstruct a geometric pattern (Špiláková, Shaw, Czekóová, & Brázdil, 2019). Employing this task within a dual-fMRI hyperscanning study, we revealed brain responses in both interactants that were contingent upon the immediately preceding behavior of their co-player. Furthermore, these brain responses dissociated among discrete dimensions of the interaction; we observed greater inter-reactive brain responses during co-operative exchanges within regions implicated in social cognition, while competitive exchanges elicited stronger brain reactions within neural systems involved in motor planning and updating. This demonstrated the potential for hyperscanning to elucidate patterns of interpersonal brain events underlying different forms of social exchange.

A number of questions emerged from these results; however, first, in an event-related design, we applied general linear modeling to identify brain signals in each player that reflected direct reactions to a specific aspect of their co-player's behavior—namely, the end point of their preceding action. As such, we observed interpersonal brain-behavior contingencies rather than brain-to-brain coupling. It remains to be seen, then, whether patterns of between-brain coupling between co-players on this task also differentiate between dissociable dimensions of social exchange. Second, by modeling brain responses to a discrete, predefined element of the players' behavior, we captured interpersonal brain-behavior relationships during an isolated snapshot of the entire social exchange. This offers limited insight into the interpersonal brain events that unfold dynamically throughout a sustained interaction, through which the nature of the exchange takes shape.

Data-driven techniques have been developed to provide an alternative way of analyzing hyperscanning data, offering a means to address these outstanding questions. By evaluating dual-fMRI data in a model-free, hypothesis-free manner, whereby no a priori assumptions are made, these techniques are more appropriate for the non-linear, unpredictable dynamic of naturalistic social exchange (Nastase, Gazzola, & Keysers, 2019). Recently, Bilek et al. (2015, 2017) demonstrated how two such data-driven techniques can be combined to investigate neural coupling during social interaction. With group-independent component analysis (gICA), one can extract spatio-temporal patterns of brain responses from a set of continuous recordings acquired from multiple interacting dyads. By assessing the dyad-specific time-course along which a given pattern is expressed, it is then possible to identify the common element of all exchanges to which those brain responses are associated; for example, one pattern might represent brain responses elicited during all instantiations of co-operative interactions, while another relates more closely to competitive exchanges. With a second model-free analytical technique—inter-subject correlation (ISC) analysis (Hasson, Nir, Levy, Fuhrmann, & Malach, 2004)—we can then investigate whether the time-course of neural signals within these data-defined patterns of interaction-specific brain responses are correlated, or aligned, between pairs of interacting individuals throughout a sustained interaction.

To examine whether dissociable patterns of neural coupling emerged during different forms of social exchange, in the present study, we applied gICA-informed ISC analysis to dual-fMRI data acquired from pairs of interactants performing our interactive task. Driven by our previous findings, we expected different patterns of neural alignment to delineate among co-operative and competitive exchanges. Furthermore, we predicted stronger alignment during concurrent relative to turn-based exchanges, given that players must monitor and adapt to their co-players' behavior in real-time during the former, giving rise to temporally coupled inter-brain contingences.

## 2 | METHODS

### 2.1 | Participants

The analyses presented below were applied to a subset of the data collected under Špiláková et al. (2019); specifically, 19 pairs of individuals who underwent the exact same dual-fMRI protocol—a necessary requirement for the analytical procedure. These 38 healthy individuals were recruited from Brno, Czech Republic. The mean age of this sample was 22.44 ( $SD = 1.90$ ) years. Participants were paired into 19 same-sex dyads (11 male–male) matched on self-evaluated handedness (34 right handers), age (mean difference = 5.79 [ $SD = 4.29$ ] months) and education (highest qualification). The individuals comprising a pair met for first time at the scanning facility on the day of the experiment and were instructed together about the task and experimental procedure. The study was approved by the Research Ethics Committee of Masaryk University, and all participants gave their informed consent prior to the scanning procedure. Participation was rewarded with 200 CZK (approximately €8).

### 2.2 | The pattern game

The pattern game is an interactive task developed originally by Decety et al. (2004), which we have adapted recently for hyperscanning research (Špiláková et al., 2019). In this game, two players either cooperate or compete with one another over recursive rounds to recreate patterns made up of blue and yellow tokens. Each player is assigned the color blue or yellow, which identifies them throughout the entire game. Prior to each round, players are shown an instruction that allocates one to the role of Builder and the second to either Helper, Hinderer, or Observer (referred to collectively as Other; e.g., “Blue builds, Yellow helps”). While the task of the Builder is always to recreate the pattern as fast as possible, the characteristics of the patterns mean that they can do so more easily with assistance from the Other. The role assigned to the Other then defined one of three conditions: during *Cooperation* rounds, they work with the Builder to help them reconstruct the pattern; in *Competition* rounds, they must work against the Builder and attempt to hinder them from achieving this. In *Control* rounds, the Other is instructed to simply observe the Builder

recreating the pattern. Players alternated between the role of Builder and Other on each round.

Players made their moves by placing tokens sequentially into specific locations of a playing board. Each round began with one of the players' tokens presented on either side of the monitor above the playing board, and using a four-button controller they moved it leftward or rightward to a desired columnar location before dropping it into the lowest empty row. On each round, both players could place up to five tokens within a time limit of 25 s. The round ended if (a) the pattern was recreated successfully, (b) both players had placed all of their tokens, or (c) 25 s had elapsed. The experiment consisted of two blocks of 48 pseudorandomized rounds: 16 *Cooperative*, 16 *Competitive*, and 16 *Control*. In the first block, participants took turns to place their tokens sequentially (*Turn-Based* condition). In the second, players were free to place their tokens simultaneously (*Concurrent* condition). Throughout a round, the Builder's token was always in the lower row, closer to the playing board; as such, if both players attempted to place their token at the same columnar position simultaneously, the Builder's token always dropped to the lowest row with the Other's token positioned above it. Figure 1 presents an overview of the task, which was programmed in MATLAB (v2018b, The MathWorks, Inc.) using the Cogent 2000 toolbox (developed by the Cogent 2000 team at the FIL and the ICN, and John Romaya at the LON at the Wellcome Department of Imaging Neuroscience; RRID:SCR\_015672).

### 2.3 | MRI data acquisition

Brain imaging was performed using two identical 3T Siemens Prisma scanners located within the same facility, both equipped with a 64-channel HeadNeck coil. First, we acquired high-resolution whole-brain T1-weighted anatomical images (MPRAGE; TR/TE/TI = 2300/2.33/900 ms; flip angle = 8°; field of view = 252 mm × 224 mm; in-plane matrix size = 252 × 224; slice thickness = 1 mm; 240 sagittal slices; iPAT GRAPPA accel. factor = 2; phase encoding = A>P; no fat suppression; acquisition time = 317 s). Functional time series were then recorded in two runs, each containing 570 volumes (approximately 20 min) acquired after four dummy scans—the turn-based block was always followed by the Concurrent block. Blood-oxygen-level dependent (BOLD) images were obtained with T2\*-weighted echo planar imaging, with parallel acquisition (i-PAT GRAPPA accel. factor = 2; 34 axial slices; TR/TE = 2000/35 ms; flip angle = 60°; field of view = 204 mm × 204 mm; in-plane matrix size = 68 × 68; slice thickness = 4 mm; 34 axial slices; phase encoding = A>P). Axial slices were acquired in interleaved order, each one oriented parallel to a line connecting the base of the cerebellum to the base of orbitofrontal cortex to ensure whole-brain coverage. A single external programmable signal generator (Siglent SDG1025, www.siglent.com) initiated the acquisition sequence of both scanners to ensure maximal synchronization (mean asynchrony in volume acquisition = 1.69 [ $SD = 0.65$ ] ms). Likewise, a single computer was used to present synchronized experimental stimuli to both scanners, and to record the timings of radio frequency pulses.

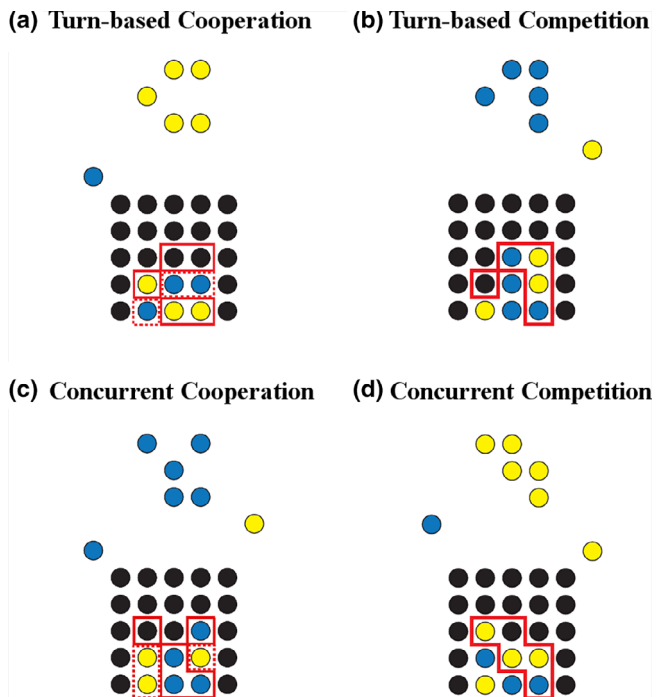


**FIGURE 1** Snapshots of stimuli during the Turn-based Cooperation (a) and Competition (b) rounds, and Concurrent Cooperation (c) and Competition (d) rounds. In all examples, the Builder is assigned to the same color as the target pattern (i.e., yellow in a and d, blue in b and c), and scores by placing tokens in locations that recreate the pattern (indicated by solid red lines). The Other is assigned to the opposing color (blue in a and d, yellow in b and c), and scores by placing their tokens in locations that serve to help or hinder the Builder (dashed red lines); since the latter is achieved by placing tokens within the pattern space, thereby obstructing the Builder, the scoring location of Others and Builders are the same in Competitive rounds (solid red lines) [Color figure can be viewed at [wileyonlinelibrary.com](http://wileyonlinelibrary.com)]

## 2.4 | Neuroimaging data analysis

The pre-processing and analysis of functional and structural brain images was performed using various utilities within FMRIB's software library (Jenkinson et al., 2012; SCR\_002823). gICA was performed using the GIFT toolbox for MATLAB (v2.0e; [mialab.mrn.org/software/gift](http://mialab.mrn.org/software/gift); Calhoun, Adali, Pearlson & Pekar, 2001), and ISC analyses were performed with in-house scripts written and executed in MATLAB (v2018b, The MathWorks, Inc.).

### 2.4.1 | Pre-processing

For each pair, we obtained four time series (two for each participant—one acquired during the *Turn-Based* block, the other during the *Concurrent* block) that were pre-processed independently in the following manner: First, slice-timing correction for interleaved slice acquisition was applied to the functional images, and each time-series was detrended and high-pass filtered across time (Gaussian-weighted least-squares straight-line fitting;  $\sigma = 50.0$  s) and spatially

smoothed with a 5-mm full-width half-maximum Gaussian kernel. Motion correction was then performed with MCFLIRT (Jenkinson et al., 2002). To remove any residual motion artifacts, or signal caused by physiological noise (e.g., heart rate and respiration), we performed single-session Independent Component Analysis with MELODIC (Beckmann & Smith, 2004) to identify 50 spatio-temporal components of the BOLD signal. Artifactual components were identified automatically using the Spatially Organized Component Klassifikator (SOCK; Bhaganagarapu et al., 2013), and any signals corresponding to these problematic components were regressed out of the time-series using *fsl\_regfilt*. Since these artifactual components were orthogonal to the signal removed previously by the high-pass filter, there was no re-introduction of noise (Lindquist, Geuter, Wager, & Caffo, 2019). In our pre-processing pipeline, the components returned by MELODIC that were identified as artifactual and subsequently regressed out of the time series (the set of nuisance covariates) were drawn from data that had been high-pass filtered already. Finally, with FLIRT, the time-series were registered to a corresponding high-resolution structural image using Boundary-based Registration, and this, in turn, was registered linearly to the Montreal Neurological Institute (MNI)-152 template (12 degrees of freedom).

### 2.4.2 | Group-independent component analysis

We performed gICA to identify common aggregate spatial maps across the entire samples that are expressed through unique time-courses for each subject. An alternative approach is to allow for unique spatial maps but common time courses, but this is less appropriate for fMRI data (see Calhoun et al. 2008).

The input consisted of 76 functional brain images (38 participants [19 pairs]  $\times$  2 blocks [*Turn-based* and *Concurrent*]), each containing 570 volumes. Two data reduction steps were first performed: principle component analysis (PCA) was applied initially to each individual time-series, resulting in a set of 68 components from each of the 76 time-series, and subsequently to all the resulting components concatenated into one matrix. The second PCA resulted in a set of 20 spatially orthogonal principal components. The optimal number of components to be extracted from each of these PCAs was determined by computing the minimum description length (MDL). The MDL principle is a formal version of Occam's razor, which determines an appropriate model complexity by extracting the maximum amount of information from the data without overfitting (Sammut & Webb, 2016). Next, spatial gICA was performed on these reduced data using the INFOMAX algorithm to identify group-level components that were independent of one another (Langlois, Chartier, & Gosselin, 2010). To ascertain the reliability of these spatial components, gICA was run 20 times and the resulting estimates were compared using ICASSO: each estimated independent component occupies one point in the signal space, and if a component is reliable then each run of the algorithm should produce one point in the signal space that is very close to the "real" component. Thus, reliable independent components correspond to clusters that are small and well separated from the rest

of the estimates. In contrast, unreliable components correspond to points which do not belong to any cluster. A cluster quality index,  $I_q$ , is then used to evaluate what clusters are the most compact and isolated; this index is computed as the difference between the average intra-cluster and average extra-cluster similarities. Eventually,  $I_q$  is equal to one for an ideal cluster (Himberg, Hyvärinen, & Esposito, 2004). This ICASSO analysis revealed that all 20 components achieved very high cluster quality indices over all iterations ( $I_q = .97-.98$ ). This part of the gICA pipeline is illustrated schematically in Figure 2a.

After visual inspection of the reliable components emerging from ICASSO, five were identified as artifactual and excluded from further analyses (e.g., components reflecting heartbeat, white matter, and cerebrospinal fluid; see Figure S1). Since the remaining 15 components were extracted from time-series acquired during cooperative *and* competitive exchanges, and in both turn-based *and* concurrent interactions, each one could express all dimensions of interaction equally or a specific dimension/combination of dimensions independently. To identify components that reflected brain responses associated with each condition (*Co-operation*, *Competition*, and *Control*), we used the results of the PCA data-reduction steps to back-reconstruct each component to the individual input time-series. This resulted in a time-course for each component specific to each subject in each block. Multiple regression analysis was then computed: For each participant, the explanatory variables were their subject-specific back-reconstructed time-course for each

independent component, and the outcome variable was their unique task design for each condition within each block. This resulted in subject-specific  $\beta$ -values for each of the three conditions during the *Concurrent* or *Turn-based* block (six  $\beta$ -values for each participant for each component). These  $\beta$ -values were then compared using paired-samples  $t$ -tests to identify interaction-specific components; that is, components for which the back-reconstructed time-course for each participant fit their task design of the experimental conditions more than the *Control* condition ( $\beta_{\text{Coop}} > 0$  and  $\beta_{\text{Coop}} > \beta_{\text{Cont}}$ ; or  $\beta_{\text{Comp}} > 0$  and  $\beta_{\text{Comp}} > \beta_{\text{Cont}}$ ), and showed greater fit for either the *Cooperation* or *Competition* condition. For components to be selected, this had to be true in both concurrent and turn-based condition. This procedure, illustrated in Figure 2b, identified four interaction-specific components.

### 2.4.3 | Inter-subject correlation analysis

Next, to calculate the degree of neural alignment in each condition we computed matrices of cross-correlations between the back-reconstructed time-series of interaction-specific components for each interacting pair, separately for the *Turn-based* and *Concurrent* block (e.g., correlation between the time-series of component #1 in the Blue player and component #2 in their Yellow co-player, in the *Turn-based* block). For each component, Pearson correlations were applied to the

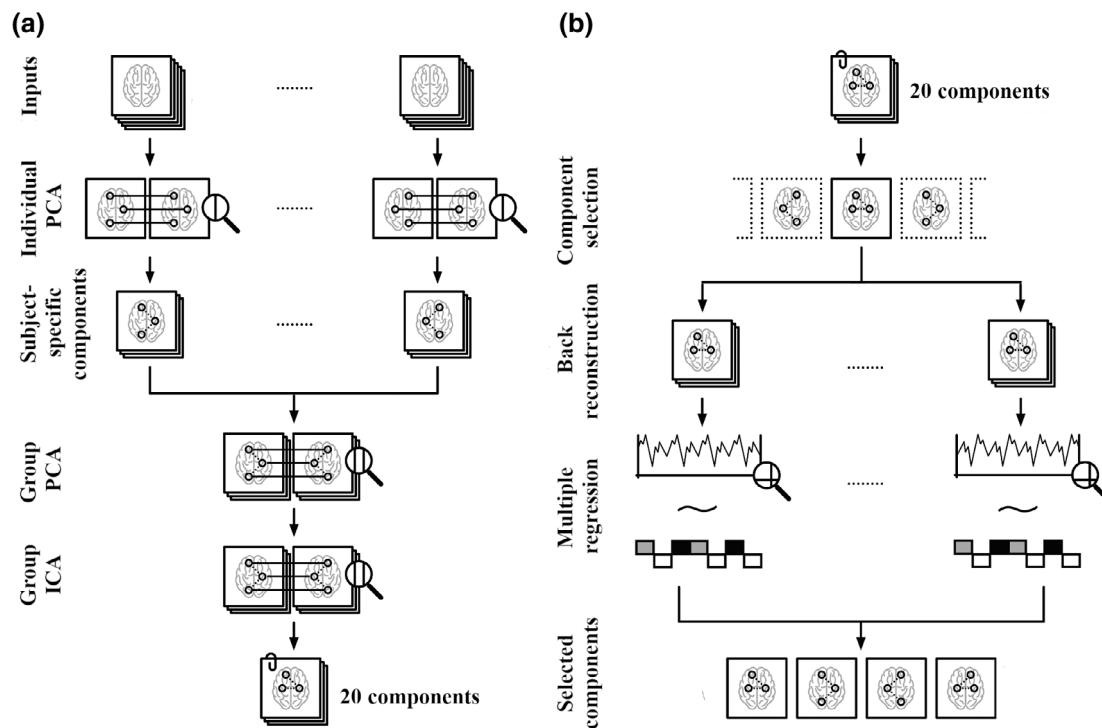


**FIGURE 2** Group-Independent Component Analysis (gICA) pipeline. (a) Two data reduction steps were performed on the pre-processed data: PCA was first applied to each individual time-series, and then to all the time-series concatenated into one matrix. Next, gICA was performed on these reduced data using the INFOMAX algorithm, revealing 20 reliable components. (b) After the removal of five artifactual components, the remaining 15 components were back-reconstructed to the individual input time-series. Applying multiple regression to the subject-specific time-series revealed four components that were expressed along a time-series aligned with interaction-specific conditions. Note: Magnifying glasses represent stages of data reduction

entire back-reconstructed time-series from within each block (570 volumes). The resulting correlation coefficients were transformed to z-values, and the median was used as a coupling coefficient. To determine the significance of the resulting coefficients, we performed a randomization test with 10,000 permutations: in each iteration, we randomly selected 38 non-interacting pairs (retaining the role of each participant; e.g., component #1 in the Blue player of one pair, and component #2 from the Yellow player of a different pair) and computed a median z-transformed coefficient as above. This produced a null distribution of correlations among non-interacting pairs for each interaction-specific component, against which the significance of coupling between each interacting pair was then compared (see Figure 4a). Pairwise comparisons among the four non-artificial, interaction-specific components revealed significantly higher correlations among interacting compared with non-interacting pairs after Bonferroni correction ( $\alpha = .05/4^2$ ). Finally, to assess whether differences existed in the strength of neural coupling between the *Concurrent* and *Turn-based* interactions, for each interaction-specific component, we compared the within-pair correlation coefficients using a Wilcoxon sign-rank test (e.g., the coefficients calculated for all interacting pairs for Component #1 in the *Turn-based* block were compared with those calculated for all interacting pairs for Component #1 in the *Concurrent* block). This analysis is illustrated in Figure 3.

While  $I_q$  obtained from ICASSO was  $>0.9$  for each cluster (component), to ensure that the individual back-reconstructed time-series were stable even with a slight change in the spatial configuration of

the component, we ran the gICA and subsequent post-processing analysis five times with the exactly same parameters. In the following section, we report only the results that were replicated in each of these five iterations.

### 3 | RESULTS

gICA revealed one component that was related more strongly to instances of the *Cooperative* compared with the *Control* rounds (component 10 in Figure S1; referred to herein as Coop#1), while three were associated more strongly with *Competitive* than *Control* rounds (components 13, 14, and 18; referred to herein as Comp#1, Comp#2, and Comp#3, respectively). The spatial pattern of brain regions comprising Coop#1 included bilateral precuneus, bilateral clusters centered on the superior temporal sulci (STS) but extending dorsally to the TPJ and ventrally to the fusiform gyri, bilateral dorso-lateral prefrontal cortices, and the cerebellum. Interestingly, Comp#1 consisted entirely of brain responses localized to the cerebellum. Those encompassed by Comp#2, however, included right precuneus, right superior frontal gyrus extending into prefrontal cortex, right caudate nucleus, right parietal inferior gyrus, and left cerebellum. In Comp#3, the brain responses were present bilaterally in superior frontal gyri, anterior cingulate cortex (ACC), anterior insulae (AI), precuneus, the cerebellum, and left precentral gyrus. These results are presented in Figure 4a.

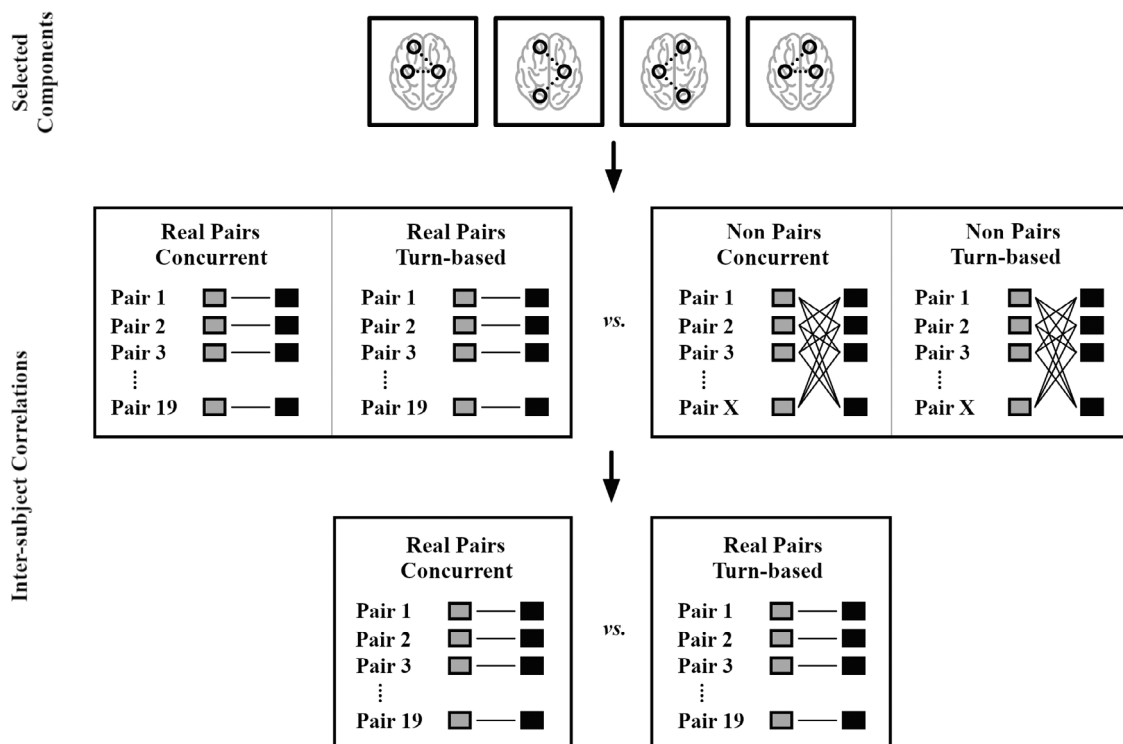


**FIGURE 3** Inter-subject correlation (ISC) pipeline. For the seven non-artificial interaction-specific components resulting from gICA, ISCs were computed for interacting pairs and compared with those between non-interacting individuals. Finally, for each component, the ISCs between interacting pairs were compared between the Turn-based and Concurrent blocks

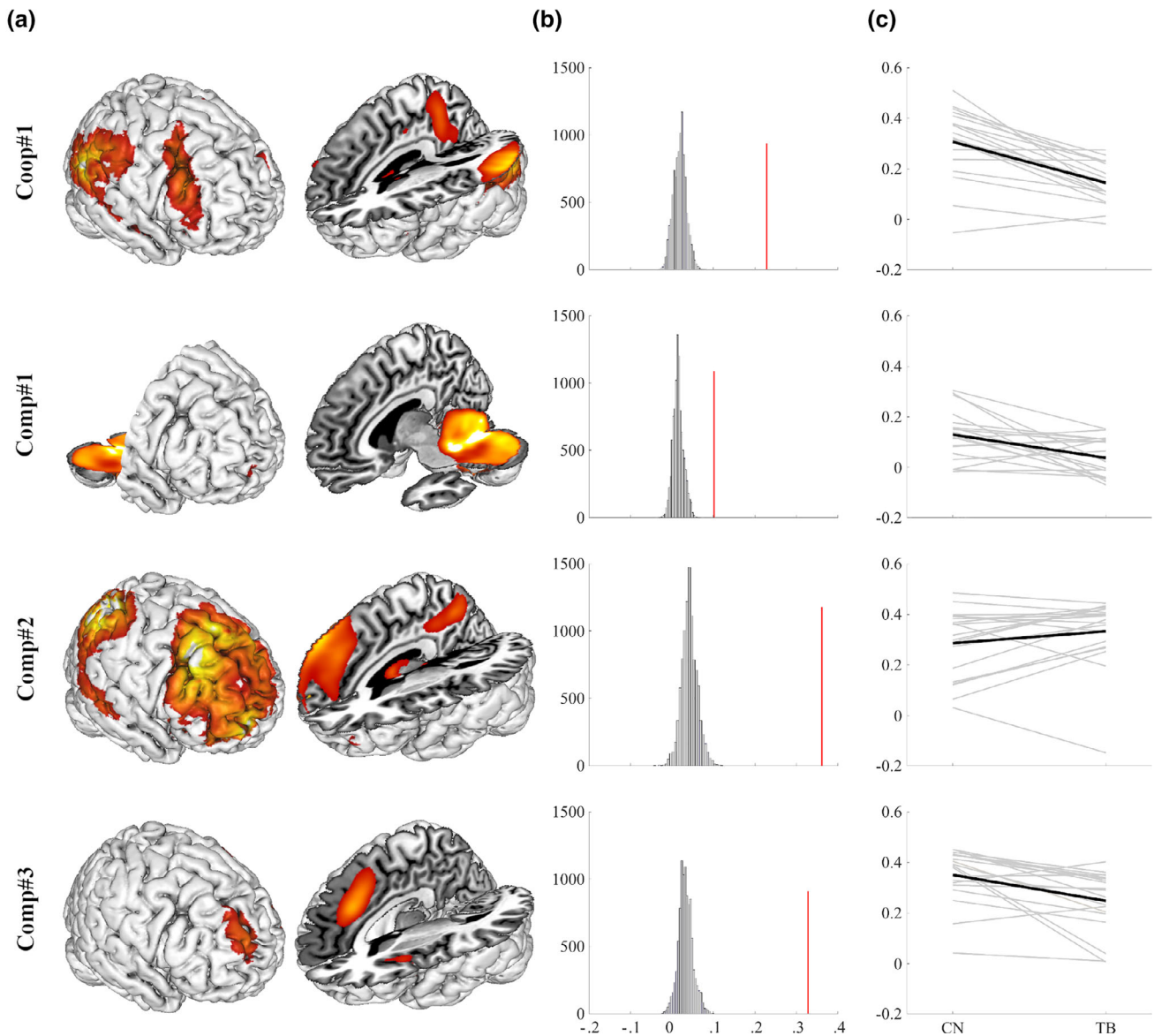


**FIGURE 4** Results of gICA-informed ISC analyses. (a) Spatial maps of four components identified by group-Independent Component Analysis (gICA), which were expressed in individual brains along time-series that corresponded to instances of cooperative or competitive interactions. (b) The randomization test revealed that the back-reconstructed time-series for each component were correlated significantly more strongly ( $p < .05$ , Bonferroni corrected) between interacting compared with non-interacting players. Histograms show the null-distribution of median correlation coefficients across all non-interacting pairs—the frequency (y-axis) with which correlations of different strengths (x-axis) were identified across all permutations. The red line presents the median correlation coefficient across all interacting pairs. (c) Comparisons between the correlation coefficients (y-axis) for all interacting pairs between the Concurrent (CN) and Turn-based (TB) blocks. Note: Components emerging from gICA are overlaid onto the Colin27 template (Holmes et al., 1998) in MNI space [Color figure can be viewed at [wileyonlinelibrary.com](http://wileyonlinelibrary.com)]

For each of these components, ISC analyses revealed that the back-reconstructed time-courses were correlated more strongly between interacting than non-interacting pairs after ( $p < .05$ , Bonferroni corrected; see Figure 4b). Furthermore, this measure of neural alignment between interacting dyads was significantly stronger during the *Concurrent* relative to the *Turn-based* block for Coop#1 (mean coupling coefficient: CN = .31 [range =  $-.05-.51$ ] vs. TB = .14 [range =  $-.02-.27$ ];  $W = 187$ ,  $Z = 3.70$ ,  $p < .001$ ), Comp#1 (mean CN = .13 [range =  $-.01-.30$ ] vs. TB = .03 [range =  $-.07-.15$ ];  $W = 161$ ,  $Z = 2.66$ ,  $p = .008$ ) and Comp#3 (CN = .35 [range =  $.04-.45$ ] vs. TB = .25 [range =  $.01-.40$ ];  $W = 176$ ,

$Z = 3.26$ ,  $p = .001$ ). For Comp#2, however, neural coupling did not differ significantly between blocks (CN = .29 [range =  $.03-.48$ ] vs. TB = .33 [range =  $-.15-.44$ ];  $W = 54$ ,  $Z = -1.65$ ,  $p = .09$ ). These results are illustrated in Figure 4c, and detailed further in Table S1.

## 4 | DISCUSSION

To investigate whether different patterns of neural coupling between individuals emerge during dissociable types of interaction, we analyzed

dual-fMRI “hyperscanning” data acquired from dyads engaged in a variety of interactions using a combination of two techniques: a data-driven gICA and subsequent ISC. This gICA-informed ISC analysis revealed a distinct spatio-temporal pattern of brain response that followed a time-course associated with co-operative exchanges, and three independent patterns that corresponded more closely to competitive interactions. More importantly, the time-courses of all these components were correlated significantly between pairs of interactants, and these distinct patterns of interpersonal brain-to-brain alignment delineated among concurrent and turn-based exchanges. These results demonstrate the utility of data-driven approaches applied to hyperscanning data in elucidating the interpersonal neural processes that give rise to the two-in-one dynamic characterizing social interaction.

Appreciating fully the ability of gICA-informed ISC analysis to distinguish among different dimensions of interpersonal interactions requires an evaluation of the analytical process: The inputs were time-series acquired during both cooperative *and* competitive conditions, and in both turn-based *and* concurrent interactions. As such, components emerging from the gICA could express all interaction dimensions equally, or a specific dimension/combination of dimensions independently. Indeed, multiple regression applied to the back-reconstructed time-series revealed that only four of the 15 non-artifactual components were specific to either cooperation or competition. By examining correlations in the time-series of these patterns across all players—both interacting *and* non-interacting pairs—we were then able to identify patterns of neural alignment that were both specific to real interactions and distinguished between co-operative and competitive exchanges performed in a concurrent or turn-based manner.

The collection of brain regions expressing interpersonal neural coupling during co-operative exchanges, Coop#1, encompassed bilateral precuneus, STS, TPJ, and the cerebellum. A substantial body of research has shown that the precuneus, STS, and TPJ comprise a network of brain regions co-activated during experimental tasks requiring the attribution of mental states to others, such as desires, intentions, and beliefs (Bardi et al., 2017; Carlson et al., 2013; Eddy, 2016). Based on its engagement during visuo-spatial mental imagery (e.g., Ghaem et al., 1997; Hanakawa et al., 2003), and both implicit and explicit mentalizing (for meta-analytic reviews, see Schilbach et al., 2012; Wolf, Dziobek, & Heekeren, 2010), it is believed that the precuneus is involved in the representation of others' perspectives (Cavanna & Trimble, 2006). Similarly, the TPJ responds when individuals are required to infer another person's perspective when it differs from their own (e.g., Dumontheil et al., 2010; Mazzarella et al., 2013); that is, when distinctions must be made between self- and other representations (Lamm, Bukowski, & Silani, 2016; Uddin, Molnar-Szakacs, Zaidel, & Iacoboni, 2006).

Since co-operative interactions require both individuals to act in line with a common goal and in a manner that complements their interaction partner's behavior (Sebanz, Bekkering, & Knoblich, 2006), it is perhaps unsurprising to observe neural alignment throughout these brain systems; both individuals must attempt to

predict their co-player's intentions and expectations in order to modify their own actions accordingly (Hampton, Bossaerts, & O'Doherty, 2008; Jara-Ettinger, Baker, & Tenenbaum, 2012; Kestemont et al., 2015; Kestemont, Vandekerckhove, Ma, Van Hoek, & Van Overwalle, 2013). Indeed, brain-to-brain synchronization within the TPJ and STS has been reported during economic exchanges (Jahng et al., 2017; Tang et al., 2016; Zhang et al., 2017), cooperative joint-action (Abe et al., 2019), and communicative tasks (Hirsch, Zhang, Noah, & Ono, 2017; Kinreich et al., 2017; Rojiani et al., 2018; Wilson et al., 2008). What is surprising, however, is the ability of a data-driven analysis to identify spatio-temporal patterns of brain response that delineate among social interactions along the goal dimension, and within which the strength of neural alignment differentiates between exchanges along the interaction dimension.

The first pattern of neural responses elicited during competitive exchanges, Comp#1, consisted exclusively of the bilateral cerebellum. An expansive corpus of research into the functions of the cerebellum points to its primary role in sensory prediction and the formation of expectations through interactions with the environment (Leggio & Molinari, 2015; Nixon, 2003). Within this pattern, neural alignment was significantly stronger during concurrent than turn-based competitive interactions. We suggest this reflects greater inter-brain contingencies in visuo-spatial processing mechanisms during real-time interaction, whereby each player must simultaneously predict and adapt to the behavior of their partner.

The second spatio-temporal pattern of brain responses elicited during competitive exchanges that were aligned between interacting players, Comp#2, comprised brain regions localized primarily to the right hemisphere, including lateral prefrontal cortex, caudate nucleus, inferior parietal cortex, and precuneus, but also the left cerebellum. The inferior parietal cortex is considered a higher-order brain area involved in the visuo-spatial control of motor behavior (Culham, Cavina-Pratesi, & Singhal, 2006; Gallivan & Culham, 2015). Given the abovementioned putative role of the cerebellum in similar motor-related spatial processing, this pattern of neural alignment might index temporally coupled dependencies in visuo-motor processes during competitive interactions. Interestingly, the caudate nucleus has been implicated in response switching (Grahn, Parkinson, & Owen, 2008), and the concerted engagement of the precuneus and the caudate nucleus has been observed during the planning and generation of strategic moves during competitive interactive games (Wan et al., 2011). Taken together, interpersonal neural coupling within this collection of brain regions might reflect the mutual recruitment of processes involved in the monitoring of a co-players behavior and subsequent updating of one's own motor actions to allow for flexible co-adaptation during competitive interactions. Importantly, while all spatio-temporal patterns were relatively unresponsive during the control condition, in which participants simply viewed the actions of their co-player, within this collection of brain regions we observed no significant differences in the strength of inter-player neural coupling between concurrent and turn-based competitive exchanges. This might reveal a pattern of alignment common to both forms of competitive interaction, allowing



individuals to plan their next move on the basis of their co-player's preceding action.

The third pattern of brain responses expressing neural alignment between players engaged in competitive interactions, Comp#3, encompassed the superior frontal cortices, ACC, AI, precuneus, and cerebellum. This converges with the findings of Wilson et al. (2008), who report ISCs of brain function during verbal communication within the ACC, lateral frontal cortices, and the precuneus. A network of frontal activations incorporating the dorsal ACC and AI constitute the so-called salience network, which is thought to be responsible for identifying behaviorally relevant stimuli. In a previous study, we observed a similar pattern of neural alignment within the dorsal ACC and AI between players involved in an interactive game of economic exchange; more specifically, inter-brain alignment in these regions was associated with the degree of reciprocity expressed between players (Shaw et al., 2018). We interpreted this to reflect the mutual effort of players to modify their own behavior according to that of their opponent, a process necessary to compete successfully in an inter-dependent context. In this light, stronger alignment with a neural saliency-detection system during concurrent compared with turn-based competitive exchanges might index a greater effort of both players to process and react dynamically to their opponent's moves; during concurrent exchanges, each player's actions present a continuous flow of salient information to their opponent, demanding more flexible co-adaptation.

Interestingly, all but one of these patterns shared a common feature—neural alignment within the precuneus. This brain region is connected reciprocally to many other parts of the brain, and is considered a member of the so-called “rich club”—a group of neural hubs that are interconnected among themselves (van den Heuvel & Sporns, 2011). Our results suggest that the precuneus plays a central role in various forms of inter-dependent social exchange; it may provide a channel through which social information is transmitted interpersonally and relayed to other brain systems to permit adaptive responses during social interaction. It is also interesting that no pattern.

These distinct patterns of brain coupling provide unique insights into the interpersonal neural processes that unfold during dissociable forms of social exchange. In three of the components identified by gICA (Coop#1, Comp#2, and Comp#3), ISCs between interacting pairs were strongest during concurrent exchanges. This converges with the results from neuroscientific investigations that have employed dual-EEG to investigate patterns of between-brain alignment during unconstrained interpersonal behavior (Dumas, Martinerie, Soussignan, & Nadel, 2012; Dumas, Nadel, Soussignan, Martinerie, & Garnero, 2010); greater inter-brain coherence is reported among interactants engaged in self-initiated, spontaneous interactions compared with exchanges that are guided externally by an experimenter—a distinction paralleling that between turn-based and concurrent exchanges. Importantly, these results do not simply reflect the degree of similarity in motoric- or sensory-related brain responses: First, inter-brain covariance was significantly stronger between pairs of interacting co-players compared with pairs of non-interacting players selected at random. Second, such interaction-specific between-brain covariance was observed in both

concurrent and turn-based exchanges—this index of neural coupling was present even when individuals took turns to observe the actions of their co-player before making a reactive response, but more so when the players reacted to one another concurrently. Third, we only extracted this index of neural coupling from within spatio-temporal patterns of brain response that followed a time-course aligned more with experimental than control rounds. During control rounds, one individual (the Builder) recreated a pattern without any help or hindrance from the Other, while the Other observed the Builder passively. Hence, ISCs were extracted from patterns of brain response elicited during inter-dependent interactions, whereby the moves of each individual were mutually dependent upon their co-player's actions. As such, stronger ISCs during concurrent compared with turn-based exchanges presumably reflects greater interpersonal neural alignment as both players monitor, evaluate, and adapt to the behavior of their co-player in real-time.

It is important to acknowledge that the results of the present study must be reproduced in larger samples before we can evaluate properly the utility of gICA-informed ISC for hyperscanning research. A more rigorous evaluation of this analytical technique also requires the present results to be reproduced with other interactive paradigms, and with designs that overcome any potential limitations of the current study. For example, dyads in our experiment always performed a block of turn-based interactions before a block of concurrent exchanges; since the concurrent condition added a level of complexity to turn-based interactions, our intention was to minimize fatigue and maximize motivation between the first- and second-half of the procedure. In doing so, however, we may have introduced order effects, and so our results require reproduction in other procedures for which such influences cannot exist.

Future research should also examine whether the interaction-specific patterns of neural coupling revealed here extend to more real-world social situations. Hyperscanning permits social neuroscience to be conducted in ecologically valid contexts; Toppi et al. (2016), for example, used dual-EEG to investigate inter-brain events among aircraft pilots during flight simulations, revealing patterns of between-brain coherence that differentiated between various cooperative scenarios. It would be interesting to see whether the same patterns of neural coupling that we have observed with our interactive experimental task delineate among social exchanges with real-world implications. Studies should also investigate if the patterns of interaction-specific coupling observed in the present study are modulated by characteristics that have been shown to alter between-brain events; should they truly reflect the social aspects of interpersonal exchanges; they should be influenced by the sex of interactants (Cheng et al., 2015) and the language used during verbal interaction (Pérez et al., 2017).

## ACKNOWLEDGMENTS

This work was supported by the European Regional Development Fund Project “National Infrastructure for Biological and Medical Imaging” (CZ.02.1.01/0.0/0.0/16 013/0001775); Ministry of Education, Youth and Sports of the Czech Republic under the Project CEITEC 2020 (LQ1601); and Czech Science Foundation (GA18-21791S). We acknowledge the core facility Multimodal and Functional Imaging Laboratory of Central European Institute of Technology supported by the

Czech-Bioluming large RI project (LM2015062 funded by MEYS CR) for their support with obtaining scientific data presented in this article. We would also like to thank Tao Liu for his assistance in the design of the experimental paradigm, and Edda Bilek for the guidance she provided in the development of the analytical pipeline.

#### DATA AVAILABILITY STATEMENT

Data are not shared, but can be made available upon request.

#### ORCID

Beáta Špiláková  <https://orcid.org/0000-0001-8132-6755>

#### REFERENCES

- Abe, M. O., Koike, T., Okazaki, S., Sugawara, S. K., Takahashi, K., Watanabe, K., & Sadato, N. (2019). Neural correlates of online cooperation during joint force production. *NeuroImage*, *191*, 150–161. <https://doi.org/10.1016/j.neuroimage.2019.02.003>
- Ahn, S., Cho, H., Kwon, M., Kim, K., Kwon, H., Kim, B. S., ... Jun, S. C. (2017). Interbrain phase synchronization during turn-taking verbal interaction—a hyperscanning study using simultaneous EEG/MEG. *Human Brain Mapping*, *39*(1), 171–188. <https://doi.org/10.1002/hbm.23834>
- Babiloni, F., & Astolfi, L. (2014). Social neuroscience and hyperscanning techniques: past, present and future. *Neuroscience & Biobehavioral Reviews*, *44*, 76–93.
- Bardi, L., Six, P., & Brass, M. (2017). Repetitive TMS of the temporoparietal junction disrupts participant's expectations in a spontaneous theory of mind task. *Social Cognitive and Affective Neuroscience*, *12*(11), 1775–1782. <https://doi.org/10.1093/scan/nsx109>
- Beckmann, C. F., & Smith, S. M. (2004). Probabilistic independent component analysis for functional magnetic resonance imaging. *IEEE Transactions on Medical Imaging*, *23*, 137–152.
- Bhaganagarapu, K., Jackson, G. D., & Abbott, D. F. (2013). An automated method for identifying artifact in independent component analysis of resting-state fMRI. *Frontiers in Human Neuroscience*, *7*(7), 1–17.
- Bilek, E., Ruf, M., Schäfer, A., Akdeniz, C., Calhoun, V. D., Schmah, C., ... Meyer-Lindenberg, A. (2015). Information flow between interacting human brains: Identification, validation, and relationship to social expertise. *Proceedings of the National Academy of Sciences*, *112*(16), 5207–5212. <https://doi.org/10.1073/pnas.1421831112>
- Bilek, E., Stöbel, G., Schäfer, A., Clement, L., Ruf, M., Robnik, L., ... Meyer-Lindenberg, A. (2017). State-dependent cross-brain information flow in borderline personality disorder. *JAMA psychiatry*, *74*(9), 949–957.
- Calhoun, V. D., Adali, T., Pearlson, G. D., & Pekar, J. J. (2001). A method for making group inferences from functional MRI data using independent component analysis. *Human brain mapping*, *14*(3), 140–151.
- Calhoun, V. D., Kiehl, K. A., & Pearlson, G. D. (2008). Modulation of temporally coherent brain networks estimated using ICA at rest and during cognitive tasks. *Human Brain Mapping*, *29*(7), 828–838.
- Carlson, S. M., Koenig, M. A., & Harms, M. B. (2013). Theory of mind. *Wiley Interdisciplinary Reviews. Cognitive Science*, *4*(4), 391–402. <https://doi.org/10.1002/wcs.1232>
- Cavanna, A. E., & Trimble, M. R. (2006). The precuneus: a review of its functional anatomy and behavioural correlates. *Brain*, *129*(3), 564–583.
- Cheng, X., Li, X., & Hu, Y. (2015). Synchronous brain activity during cooperative exchange depends on gender of partner: A fNIRS-based hyperscanning study. *Human Brain Mapping*, *36*(6), 2039–2048. <https://doi.org/10.1002/hbm.22754>
- Culham, J. C., Cavina-Pratesi, C., & Singhal, A. (2006). The role of parietal cortex in visuomotor control: What have we learned from neuroimaging? *Neuropsychologia*, *44*(13), 2668–2684. <https://doi.org/10.1016/j.neuropsychologia.2005.11.003>
- Decety, J., Jackson, P. L., Sommerville, J. A., Chaminade, T., & Meltzoff, A. N. (2004). The neural bases of cooperation and competition: an fMRI investigation. *NeuroImage*, *23*, 744–751.
- Dumas, G., Martinerie, J., Soussignan, R., & Nadel, J. (2012). Does the brain know who is at the origin of what in an imitative interaction? *Frontiers in Human Neuroscience*, *6*, 1–11. <https://doi.org/10.3389/fnhum.2012.00128>
- Dumas, G., Nadel, J., Soussignan, R., Martinerie, J., & Garnero, L. (2010). Inter-brain synchronization during social interaction. *PLoS One*, *5*(8), e12166. <https://doi.org/10.1371/journal.pone.0012166>
- Dumontheil, I., Küster, O., Apperly, I. A., & Blakemore, S. J. (2010). Taking perspective into account in a communicative task. *NeuroImage*, *52*(4), 1574–1583.
- Eddy, C. M. (2016). The junction between self and other? Temporoparietal dysfunction in neuropsychiatry. *Neuropsychologia*, *89*, 465–477. <https://doi.org/10.1016/j.neuropsychologia.2016.07.030>
- Frith, C. D., & Frith, U. (2006). The neural basis of Mentalizing. *Neuron*, *50*(4), 531–534. <https://doi.org/10.1016/j.neuron.2006.05.001>
- Gallivan, J. P., & Culham, J. C. (2015). Neural coding within human brain areas involved in actions. *Current Opinion in Neurobiology*, *33*, 141–149. <https://doi.org/10.1016/j.conb.2015.03.012>
- Ghaem, O., Mellet, E., Crivello, F., Tzourio, N., Mazoyer, B., Berthoz, A., & Denis, M. (1997). Mental navigation along memorized routes activates the hippocampus, precuneus, and insula. *Neuroreport*, *8*(3), 739–744.
- Grahn, J. A., Parkinson, J. A., & Owen, A. M. (2008). The cognitive functions of the caudate nucleus. *Progress in Neurobiology*, *86*(3), 141–155. <https://doi.org/10.1016/j.pneurobio.2008.09.004>
- Hampton, A. N., Bossaerts, P., & O'Doherty, J. P. (2008). Neural correlates of mentalizing-related computations during strategic interactions in humans. *Proceedings of the National Academy of Sciences*, *105*(18), 6741–6746.
- Hanakawa, T., Honda, M., Okada, T., Fukuyama, H., & Shibasaki, H. (2003). Neural correlates underlying mental calculation in abacus experts: a functional magnetic resonance imaging study. *NeuroImage*, *19*(2), 296–307.
- Hari, R., Himberg, T., Nummenmaa, L., Hämäläinen, M., & Parkkonen, L. (2013). Synchrony of brains and bodies during implicit interpersonal interaction. *Trends in Cognitive Sciences*, *17*(3), 105–106. <https://doi.org/10.1016/j.tics.2013.01.003>
- Hasson, U., & Frith, C. D. (2016). Mirroring and beyond: Coupled dynamics as a generalized framework for modelling social interactions. *Philosophical Transactions of the Royal Society B: Biological Sciences*, *371*(1693), 20150366. <https://doi.org/10.1098/rstb.2015.0366>
- Hasson, U., & Honey, C. J. (2012). Future trends in neuroimaging: Neural processes as expressed within real-life contexts. *NeuroImage*, *62*(2), 1272–1278. <https://doi.org/10.1016/j.neuroimage.2012.02.004>
- Hasson, U., Nir, Y., Levy, I., Fuhrmann, G., & Malach, R. (2004). Intersubject synchronization of cortical activity during natural vision. *Science (New York, NY)*, *303*(2004), 1634–1640. <https://doi.org/10.1126/science.1089506>
- Himberg, J., Hyvärinen, A., & Esposito, F. (2004). Validating the independent components of neuroimaging time series via clustering and visualization. *NeuroImage*, *22*(3), 1214–1222. <https://doi.org/10.1016/j.neuroimage.2004.03.027>
- Hirsch, J., Zhang, X., Noah, J. A., & Ono, Y. (2017). Frontal temporal and parietal systems synchronize within and across brains during live eye-to-eye contact. *NeuroImage*, *157*, 314–330. <https://doi.org/10.1016/j.neuroimage.2017.06.018>
- Holmes, C. J., Hoge, R., Collins, L., Woods, R., Toga, A. W., & Evans, A. C. (1998). Enhancement of MR images using registration for signal averaging. *Journal of Computer Assisted Tomography*, *22*, 324–333. <https://doi.org/10.1097/00004728-199803000-00032>

- Jahng, J., Kralik, J. D., Hwang, D. U., & Jeong, J. (2017). Neural dynamics of two players when using nonverbal cues to gauge intentions to cooperate during the Prisoner's dilemma game. *NeuroImage*, *157*, 263–274. <https://doi.org/10.1016/j.neuroimage.2017.06.024>
- Jara-Ettinger, J., Baker, C., & Tenenbaum, J. (2012). Learning what is where from social observations. *Proceedings of the Annual Meeting of the Cognitive Science Society*, *34*(34), 515–520.
- Jenkinson, M., Bannister, P. R., Brady, J. M., & Smith, S. M. (2002). Improved optimisation for the robust and accurate linear registration and motion correction of brain images. *NeuroImage*, *17*(2), 825–841.
- Jenkinson, M., Beckmann, C. F., Behrens, T. E. J., Woolrich, M. W., & Smith, S. M. (2012). FSL. *NeuroImage*, *62*(2), 782–790.
- Kasai, K., Fukuda, M., Yahata, N., Morita, K., & Fujii, N. (2015). The future of real-world neuroscience: Imaging techniques to assess active brains in social environments. *Neuroscience Research*, *90*, 65–71. <https://doi.org/10.1016/j.neures.2014.11.007>
- Kestemont, J., Ma, N., Baetens, K., Clément, N., Van Overwalle, F., & Vandekerckhove, M. (2015). Neural correlates of attributing causes to the self, another person and the situation. *Social Cognitive and Affective Neuroscience*, *10*(1), 114–121. <https://doi.org/10.1093/scan/nsu030>
- Kestemont, J., Vandekerckhove, M., Ma, N., Van Hoeck, N., & Van Overwalle, F. (2013). Situation and person attributions under spontaneous and intentional instructions: An fMRI study. *Social Cognitive and Affective Neuroscience*, *8*(5), 481–493. <https://doi.org/10.1093/scan/nss022>
- Kinreich, S., Djalovski, A., Kraus, L., Louzoun, Y., & Feldman, R. (2017). Brain-to-brain synchrony during naturalistic social interactions. *Scientific Reports*, *7*(1), 17060. <https://doi.org/10.1038/s41598-017-17339-5>
- Koike, T., Tanabe, H. C., & Sadato, N. (2015). Hyperscanning neuroimaging technique to reveal the “two-in-one” system in social interactions. *Neuroscience Research*, *90*, 25–32. <https://doi.org/10.1016/j.neures.2014.11.006>
- Konvalinka, I., & Roepstorff, A. (2012). The two-brain approach: How can mutually interacting brains teach us something about social interaction? *Frontiers in Human Neuroscience*, *6*, 1–10. <https://doi.org/10.3389/fnhum.2012.00215>
- Lamm, C., Bukowski, H., & Silani, G. (2016). From shared to distinct self-other representations in empathy: Evidence from neurotypical function and socio-cognitive disorders. *Philosophical Transactions of the Royal Society B: Biological Sciences*, *371*(1686), 20150083. <https://doi.org/10.1098/rstb.2015.0083>
- Langlois, D., Chartier, S., & Gosselin, D. (2010). An introduction to independent component analysis: InfoMax and FastICA algorithms. *Tutorials in Quantitative Methods for Psychology*, *6*(1), 31–38. <https://doi.org/10.20982/tqmp.06.1.p031>
- Leggio, M., & Molinari, M. (2015). Cerebellar sequencing: A trick for predicting the future. *The Cerebellum*, *14*(1), 35–38. <https://doi.org/10.1007/s12311-014-0616-x>
- Lindquist, M. A., Geuter, S., Wager, T. D., & Caffo, B. S. (2019). Modular preprocessing pipelines can reintroduce artifacts into fMRI data. *Human brain mapping*, *40*(8), 2358–2376.
- Liu, T., & Pelowski, M. (2014). Clarifying the interaction types in two-person neuroscience research. *Frontiers in Human Neuroscience*, *8*, 276. <https://doi.org/10.3389/fnhum.2014.00276>
- Mazzarella, E., Ramsey, R., Conson, M., & Hamilton, A. (2013). Brain systems for visual perspective taking and action perception. *Social neuroscience*, *8*(3), 248–267.
- Nastase, S. A., Gazzola, V., & Keysers, C. (2019). Measuring shared responses across subjects using intersubject correlation. *Social Cognitive and Affective Neuroscience*, *14*(6), 667–685. <https://doi.org/10.1101/600114>
- Nixon, P. D. (2003). The role of the cerebellum in preparing responses to predictable sensory events. *Cerebellum*, *2*(2), 114–122. <https://doi.org/10.1080/14734220310011353>
- Pérez, A., Carreiras, M., & Duñabeitia, J. A. (2017). Brain-to-brain entrainment: EEG interbrain synchronization while speaking and listening. *Scientific Reports*, *7*(1), 1–12. <https://doi.org/10.1038/s41598-017-04464-4>
- Pérez, A., Dumas, G., Karadag, M., & Duñabeitia, J. A. (2019). Differential brain-to-brain entrainment while speaking and listening in native and foreign languages. *Cortex*, *111*, 303–315.
- Redcay, E., & Schilbach, L. (2019). Using second-person neuroscience to elucidate the mechanisms of social interaction. *Nature Reviews Neuroscience*, *20*, 495–505. <https://doi.org/10.1038/s41583-019-0179-4>
- Rojiani, R., Zhang, X., Noah, A., & Hirsch, J. (2018). Communication of emotion via drumming: Dual-brain imaging with functional near-infrared spectroscopy. *Social Cognitive and Affective Neuroscience*, *13*(10), 1047–1057. <https://doi.org/10.1093/scan/nsy076>
- Sammut, C., & Webb, G. I. (2016). In C. Sammut & G. I. Webb (Eds.), *Encyclopedia of machine learning and data mining*. Boston, MA: Springer US. <https://doi.org/10.1007/978-1-4899-7502-7>
- Sänger, J., Müller, V., & Lindenberger, U. (2012). Intra- and interbrain synchronization and network properties when playing guitar in duets. *Frontiers in Human Neuroscience*, *6*, 312. <https://doi.org/10.3389/fnhum.2012.00312>
- Schilbach, L., Bzdok, D., Timmermans, B., Fox, P. T., Laird, A. R., Vogeley, K., & Eickhoff, S. B. (2012). Introspective minds: Using ALE meta-analyses to study commonalities in the neural correlates of emotional processing, social & unconstrained cognition. *PLoS One*, *7*(2), e30920. <https://doi.org/10.1371/journal.pone.0030920>
- Schilbach, L., Timmermans, B., Reddy, V., Costall, A., Bente, G., Schlicht, T., & Vogeley, K. (2013). Toward a second-person neuroscience. *Behavioral and Brain Sciences*, *36*(04), 393–414. <https://doi.org/10.1017/S0140525X12000660>
- Scholkman, F., Holper, L., Wolf, U., & Wolf, M. (2013). A new methodical approach in neuroscience: assessing inter-personal brain coupling using functional near-infrared imaging (fNIRI) hyperscanning. *Frontiers in human neuroscience*, *7*, 813.
- Sebanz, N., Bekkering, H., & Knoblich, G. (2006). Joint action: Bodies and minds moving together. *Trends in Cognitive Sciences*, *10*, 70–76. <https://doi.org/10.1016/j.tics.2005.12.009>
- Shaw, D. J., Czekóová, K., Staněk, R., Mareček, R., Urbánek, T., Špalek, J., ... Brázdil, M. (2018). A dual-fMRI investigation of the iterated ultimatum game reveals that reciprocal behaviour is associated with neural alignment. *Scientific Reports*, *8*(1), 10896. <https://doi.org/10.1038/s41598-018-29233-9>
- Špiláková, B., Shaw, D. J., Czekóová, K., & Brázdil, M. (2019). Dissecting social interaction: Dual-fMRI reveals patterns of interpersonal brain-behavior relationships that dissociate among dimensions of social exchange. *Social Cognitive and Affective Neuroscience*, *14*(2), 225–235. <https://doi.org/10.1093/scan/nsz004>
- Tang, H., Mai, X., Wang, S., Zhu, C., Krueger, F., & Liu, C. (2016). Interpersonal brain synchronization in the right temporo-parietal junction during face-to-face economic exchange. *Social Cognitive and Affective Neuroscience*, *11*(1), 23–32. <https://doi.org/10.1093/scan/nsv092>
- Toppi, J., Borghini, G., Petti, M., He, E. J., De Giusti, V., ... Babiloni, F. (2016). Investigating cooperative behavior in ecological settings: An EEG Hyperscanning study. *PLOS One*, *11*(4), e0154236. <https://doi.org/10.1371/journal.pone.0154236>
- Uddin, L. Q., Molnar-Szakacs, I., Zaidel, E., & Iacoboni, M. (2006). rTMS to the right inferior parietal lobule disrupts self-other discrimination. *Social Cognitive and Affective Neuroscience*, *1*(1), 65–71. <https://doi.org/10.1093/scan/nsl003>
- van den Heuvel, M. P., & Sporns, O. (2011). Rich-Club Organization of the Human Connectome. *Journal of Neuroscience*, *31*(44), 15775–15786. <https://doi.org/10.1523/JNEUROSCI.3539-11.2011>
- Wan, X., Nakatani, H., Ueno, K., Asamizuya, T., Cheng, K., & Tanaka, K. (2011). The neural basis of intuitive best next-move generation in board game experts. *Science*, *331*(6015), 341–346. <https://doi.org/10.1126/science.1194732>

- Wilson, S. M., Molnar-Szakacs, I., & Iacoboni, M. (2008). Beyond superior temporal cortex: Intersubject correlations in narrative speech comprehension. *Cerebral Cortex*, *18*, 230–242. <https://doi.org/10.1093/cercor/bhm049>
- Wolf, I., Dziobek, I., & Heekeren, H. R. (2010). Neural correlates of social cognition in naturalistic settings: A model-free analysis approach. *NeuroImage*, *49*(1), 894–904. <https://doi.org/10.1016/j.neuroimage.2009.08.060>
- Zaki, J., Bolger, N., & Ochsner, K. (2008). The Interpersonal Nature of Empathic Accuracy. *Psychological Science*, *19*(4), 399–404.
- Zhang, M., Liu, T., Pelowski, M., Jia, H., & Yu, D. (2017). Social risky decision-making reveals gender differences in the TPJ: A hyper-scanning study using functional near-infrared spectroscopy. *Brain and Cognition*, *119*, 54–63. <https://doi.org/10.1016/j.bandc.2017.08.008>

## SUPPORTING INFORMATION

Additional supporting information may be found online in the Supporting Information section at the end of this article.

**How to cite this article:** Špiláková B, Shaw DJ, Czekóová K, Mareček R, Brázdil M. Getting into sync: Data-driven analyses reveal patterns of neural coupling that distinguish among different social exchanges. *Hum Brain Mapp*. 2019;1–12. <https://doi.org/10.1002/hbm.24861>